Bull. Mater. Sci. (2019) 42:191
https://doi.org/10.1007/s12034-019-1882-5

Exhibition of polarization conversions with asymmetric transmission theory, natural like chiral, artificial chiral nihility and retrieval studies for K- and C-band radar applications

OĞUZ DERİN[1], MUHARREM KARAASLAN[2,*], EMİN ÜNAL[2], FARUK KARADAĞ[3], OLCAY ALTINTAŞ[2] and OĞUZHAN AKGÖL[2]

[1]Vocational School of Technical Sciences, Mersin University, Mersin 33290, Turkey
[2]Department of Electrical and Electronics Engineering, Iskenderun Technical University, Hatay 31200, Turkey
[3]Department of Physics, Çukurova University, Adana 01330, Turkey
*Author for correspondence (muharrem.karaaslan@iste.edu.tr)

MS received 10 December 2018; accepted 3 March 2019; published online 14 June 2019

Abstract. In this study, asymmetric transmission, natural chirality phenomena and a retrieval study with chiral metamaterials (MTMs) are numerically and experimentally focussed, investigated and discussed by examining the polarization conversion effect. Suggested multi-functional designs have simple geometries (π-shaped), low losses and huge optical activities. In addition, these new designs are numerically and experimentally retrieved in the study. The proposed model has many advantages with respect to the asymmetric transmission and chiral MTM studies in the literature. These advantages are having simple geometries (π-shaped), large asymmetric transmissions, small chirality like natural materials and also huge chirality can also be provided by rotating one of the resonators. Besides, the proposed structure can be easily reconfigured for other frequency regimes to provide new chiral MTMs or can be adopted for different application areas from defence systems to stealth technology which will be examined in our future studies.

Keywords. MTMs; asymmetric transmission; natural chirality.

1. Introduction

Metamaterials (MTMs) have attracted a great interest by the electromagnetic (EM) science and community due to unnatural EM features like negative refraction [1]. These man-made materials can be designed for any desired frequency range from the radio to near optical spectrum [2–8]. They also have many application areas such as cloaking, super lens, absorber and so on [9–11]. Nowadays, the concept of chiral MTMs has rapidly repealed considerable attention of researchers due to their unnatural EM features, such as circular dichroism [2], optical activity [1] and negative refraction [3] which are not seen in conventional materials. They are artificial and hand-made structures. Therefore, they can be designed for any desired frequency regimes and have potential applications depending on manufacturing capability. They are represented with the chirality parameter κ, which can be found as $\kappa = (n_R - n_L)/2$, where n_R and n_L are the refractive index of the right and left circularly polarized (RCP and LCP) waves, respectively [4–13]. There are many chiral MTM studies in the literature, but unlike the others, in this study, we present simple design (π-shaped), easy fabrication, large optical activity, circular dichroism, chiral nihility and constant value of chirality in a wide band by using two π-shaped periodic structures. There is no other study which realizes all of these properties with a couple of asymmetric inclusions, especially, constant chirality in a wide band frequency range and chiral nihility MTMs.

The importance of the small chirality is its negligible effect on the effective refractive index. Especially, in some particular multilayer bulk chiral applications, such as filtering and polarization rotation, small chirality values with respect to the upper limits are required. The MTMs with constant small chirality gives opportunity to design microwave filters and polarizers within a wide frequency range. In the case of using double-negative MTMs or single-negative MTMs, it is not possible to provide this effect [14]. In contrast to chiral MTMs, DNG-MTM-based multilayer structures lose polarization rotation properties and behave as a narrow band filter. Another application of asymmetric transmission is diffraction on photonic crystals with wideband and switchable transmission properties [15,16]. There are many natural chiral materials, such as sugar, liquid crystals, etc. in the environment. Chirality admittances of the natural chiral materials are very small with respect to the artificially designed-chiral materials investigated by researchers. However, up to now, chirality properties of these materials have not been investigated by researchers. Handedness is necessarily intrinsic for chiral materials. In contrast to these natural chiral materials, conventional chiral MTMs are artificial structures. The advantage of the artificial chiral medium is to provide a determinable frequency and range for different application areas.

In this study, asymmetric transmission features of chiral MTMs composed of simple (π-shaped) design are proposed, retrieved and studied. These materials are made up of unit cells without mirror symmetry and can be used to manipulate the polarization states of EM waves in any desired case, either vertical or horizontal polarization states. In this regard, we theoretically and numerically investigated the asymmetric transmission phenomenon for linearly polarized EM waves by using a new design of chiral MTMs. The proposed models have many advantages, such as very simple geometry, large asymmetric transmission, polarization rotation, small chirality like natural material (also huge chirality as desired with the feature of mechanical tunability) and so on.

2. Asymmetric transmission phenomenon for linearly polarized EM waves

2.1 *Theoretical analysis*

Asymmetric transmission with chiral MTMs is provided by exhibition of the polarization conversion effect. This phenomenon is realized with an EM wave–matter interaction and the existence of a static magnetization of any medium composed of chiral MTMs. Firstly, theoretical calculations for asymmetric transmission are described by the electric field and transmission coefficients (illustrated in equations (1 and 2), respectively) in terms of the incident and transmitted electric field radiations. Secondly, we assumed an incoming plane wave that propagates in $+z$ direction with a time dependence of e^{-iwt} for the incident and transmitted electric field radiations [17–20].

$$E_{\mathrm{i}}(r,t) = \begin{pmatrix} E_x \\ E_y \end{pmatrix} e^{ikz}, \tag{1}$$

$$E_{\mathrm{t}}(r,t) = \begin{pmatrix} T_x \\ T_y \end{pmatrix} e^{ikz}, \tag{2}$$

where E_x, E_y and T_x, T_y represent complex amplitudes of EM waves and ω and k correspond to the angular frequency and wave vector, respectively. In addition, the transmission matrix given in equation (3) defines the complex amplitudes of the transmitted field in terms of the incident electric field.

$$\begin{pmatrix} T_x \\ T_y \end{pmatrix} = \begin{pmatrix} T_{xx} & T_{xy} \\ T_{yx} & T_{yy} \end{pmatrix} \begin{pmatrix} E_x \\ E_y \end{pmatrix} = \hat{T}^{f}_{\mathrm{lin}} \begin{pmatrix} E_x \\ E_y \end{pmatrix}, \tag{3}$$

where f and lin represent propagation in the forward direction and a special linear base with base vectors parallel to the coordinate axes (i.e., decomposed parts of the incident wave into x- and y-polarized components). The transmitted co-polar EM waves in the x and y directions are T_{xx} and T_{yy}, respectively. Circularly polarized-transmitted waves can be retrieved from the linear cross-polar transmission coefficients of T_{xy} and T_{yx}, respectively. Besides, they can be defined as $T_{\pm} = T_{xx} \pm i T_{yx}$. Circular transmission coefficients (T_{++}, T_{-+}, T_{+-} and T_{--}) can be calculated from the transmission coefficients of linearly polarized waves by using equations (4 and 5) in the $\pm z$ direction [13,17–21]:

$$T^{f}_{\mathrm{circ}} = \begin{pmatrix} T_{++} & T_{+-} \\ T_{-+} & T_{--} \end{pmatrix}, \quad T^{b}_{\mathrm{circ}} = \begin{pmatrix} T_{++} & T_{-+} \\ T_{+-} & T_{-} \end{pmatrix}. \tag{4}$$

If the propagation of the EM wave is along the $-z$ direction, the circularly transmitted wave components can be evaluated by using the equation below:

$$\begin{pmatrix} T_{++} & T_{\pm} \\ T_{\mp} & T_{-} \end{pmatrix} = 1/2 \begin{pmatrix} T_{xx} + T_{yy} + i\left(T_{xy} - T_{yx}\right) & T_{xx} - T_{yy} + i\left(T_{xy} + T_{yx}\right) \\ T_{xx} - T_{yy} - i\left(T_{xy} + T_{yx}\right) & T_{xx} + T_{yy} - i\left(T_{xy} - T_{yx}\right) \end{pmatrix}. \tag{5}$$

A parameter of Δ is often used to quantitate the effect of asymmetric transmission of the linearly and circularly polarized-EM waves. This is defined as $\Delta^{(x)}_{\mathrm{lin}} = \left|T_{yx}\right|^2 - \left|T_{xy}\right|^2 = -\Delta^{(y)}_{\mathrm{lin}}$, $\Delta^{(x)}_{\mathrm{circ}} = |T_{-+}|^2 - |T_{+-}|^2 = -\Delta^{(y)}_{\mathrm{circ}}$ for linearly and circularly polarized waves, respectively. The indices of circ and lin indicate propagation in circularly polarized waves and a special linear base with base vectors parallel to the coordinate axes (i.e., decomposing the incident wave into x and y polarized components).

2.2 *Proposed design and numerical setup*

The suggested chiral MTM design consists of π-shaped resonators on one side and rotated (180°) version of the same shape on the back-side as shown in figure 1a. In addition, numerical calculations are analysed with a commercial simulation software (CST Microwave Studio) based on the finite integration technique to determine the reflection and transmission properties of the proposed chiral MTM design. Unit cell ($x-y$) and open add space (z) boundary conditions are assigned in the simulation to provide periodicity as shown in figure 1b. Metallic resonators are modelled as a copper sheet with an electrical conductivity of 5.8001×10^7 S m^{-1} and a thickness of 0.035 mm. FR4 is chosen as the dielectric substrate, a high frequency laminate with a thickness of 1.6 mm, relative permittivity of 4.2, permeability of 1 and loss tangent of 0.02. FR4 has been chosen due to its low cost and easy fabrication process. Besides, figure 1c shows the dimensions of the unit cell for the proposed structure.

2.3 *Numerical study for natural chirality with large asymmetric transmission phenomena (8–24 GHz regime)*

The obtained results are presented to demonstrate the performance and frequency response of the proposed structure with large asymmetric transmission. The proposed chiral

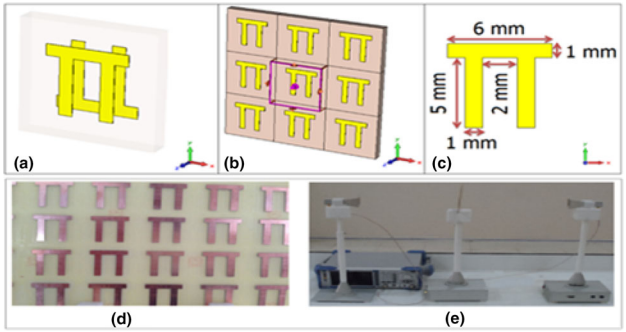

Figure 1. The suggested chiral MTM: (**a**) schematic view of the unit cell, (**b**) boundary conditions, (**c**) resonator dimensions and (**d**) fabricated chiral MTM for natural chirality and (**e**) an image of the measurement setup.

MTM geometry is designed and simulated with respect to the plane EM waves propagating along $(+z)$ and $(-z)$ directions. Then, linear transmission matrix coefficients of the slab are obtained for the x-polarized-incident EM wave. In addition, y-polarized T_{xy} and T_{yy} linear transmission matrix coefficients of the slab are found to obtain asymmetric transmission calculations. The asymmetric transmission parameter, Δ, is calculated by using a theoretical approach and normalized for both linear and circular polarization cases as shown in figure 2. It can be understood that the suggested structure shows multi-band asymmetric transmission at resonance frequencies of 10.85, 14.49 and 14.88 GHz for linear polarization. The parameter Δ reaches its maximum value at the resonance frequency of 14.49 GHz. The asymmetry can also be exhibited from the simulated chirality admittance (figure 2).

The eigenstates and optical and EM properties of the bi-isotropic structures [22] (right circular polarized (RCP) and left circular polarized (LCP)) can be evaluated by using retrieval formulae based on S parameters. They can also be retrieved by using the standard equations for the anisotropic and bi-anisotropic media [23–27]. Although the proposed π-shapes are not isotropic, the retrieval procedure for chiral MTMs can be used due to the asymmetric geometry of the π-shaped pairs placed top and bottom surfaces of FR4 similar to the asymmetric chiral cross-wire stripes [24]. Also, we retrieved the proposed model to show natural chirality feature which is realized for the polarization rotator, EM filter and coating applications. Chirality can be retrieved directly from the transmission coefficients as [18–20,23,24]:

$$\mathrm{Re}\,(\kappa) = \frac{\left[\arg\,(T+) - \arg\,(T-) + 2m\pi\right]}{2k_0 d}, \tag{6a}$$

$$\mathrm{Im}\,(\kappa) = \frac{\ln|T_\mathrm{L}| - \ln|T_\mathrm{R}|}{2k_0 d}, \tag{6b}$$

where k_0 is the wave vector in the vacuum, d is the thickness of the structure and m can be any integer to provide physically

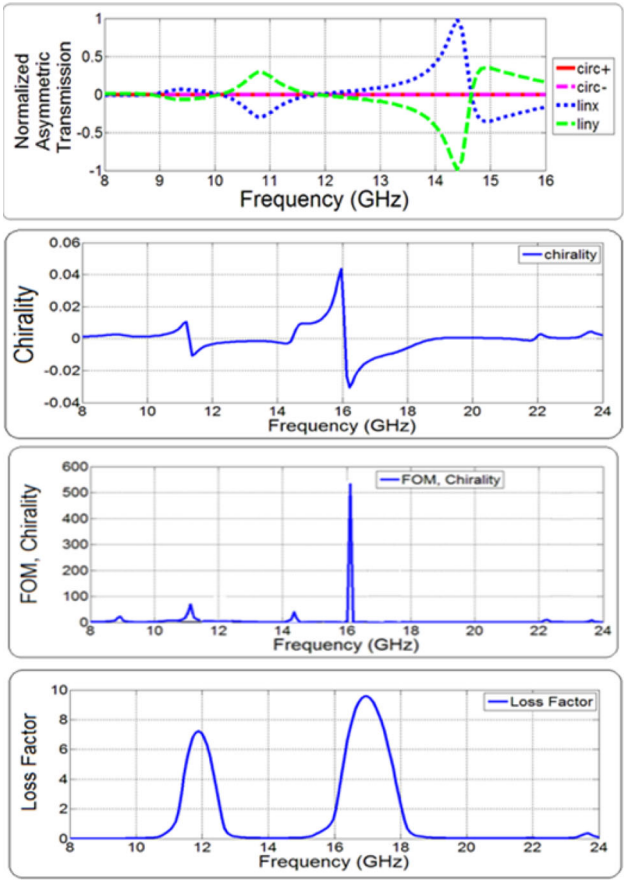

Figure 2. Simulated asymmetric transmission parameter for linear and circular polarizations, chirality parameter, FOM value and LF of the suggested structure, respectively.

meaningful results [25,28,29]. The retrieved chirality parameter is shown in figure 2 to show natural chirality phenomena. It can be seen that the proposed structure has a small-natural chirality value and it reaches the maximum value at the frequency of 16 GHz. In fact, chiral MTM studies generally focus on large chirality values for huge optical activity. However, chiral MTMs which have small chirality have not queried in the literature up to now and it is mostly ignored by researchers. Small chirality provides manipulation of the transmitted EM wave throughout rotation of polarization. The value of the chirality is directly related to the angle of the π-shape on the backside. π-shaped inclusions result in natural chirality for 0 and 180°, strong chirality can be achieved by increasing asymmetry between π-shaped resonators placed at front- and back-sides. This is proved in the retrieval study part. The reason is that the optimum chirality value provides perfect symmetry in the reflection and transmission of an EM wave in the operation frequency range. However, the symmetry can be lost for different chirality values. Besides, chirality values at the resonance frequencies also confirm the asymmetric behaviour of the structure. In addition, figure of merit $(\mathrm{FOM}) = \mathrm{Re}(\kappa)/\mathrm{Im}\,(\kappa)$ is also calculated and presented for

chirality to show that the proposed chiral MTM shows very low loss according to the many presented chiral MTMs as shown in figure 2 [25,28,29]. The high values of the FOM around peak values of chirality exhibit the acceptability of the performance of the structure. Losses in any dielectric and magnetic mediums can be obtained by a ratio of an imaginary part and a real part of permittivity and permeability. Therefore, if any medium is considered, both material parameters should be taken into consideration [30]. It is well known fact that the ratios of imaginary and real parts of both permittivity and permeability in dielectric and magnetic media represent losses of the structure [31]. Hence, if the medium properties are not exactly known, i.e., dielectric and/or magnetic ones, the loss of the medium can only be determined by using both the parameters. The easiest way is to evaluate the ratio of the imaginary and real parts of the refractive index which includes both permittivity and permeability [32]. Whereas, the real part of the refractive index denotes an ordinary value and the imaginary part defines the absorption and attenuation properties of the related medium. Hence, the loss of the chiral medium is represented by the equation of the loss factor (LF) $= \left|n''/n'\right|$, where n'' is the ratio of its imaginary part and n' is the real part of a refractive index. The obtained LFs are acceptable for the peak chirality values (figure 2). The LFs at the peak points of chirality are < 1 and both FOM and LF results prove that the proposed structure can be preferred to the design asymmetric transmitter and polarization converter with low loss at the resonance frequencies.

2.4 *Numerical and experimental study for natural chirality with large asymmetric transmission phenomena (4–6 GHz regime)*

The same procedures have been applied for higher dimensions of the π-shaped structure to exhibit both the agreement of the measurement-simulation results and applicability between 4–6 GHz regimes. The proposed structure has been manufactured by using the LPKF prototyping machine. A double copper-sided FR4 type dielectric substrate with a dielectric layer thickness of 1.6 mm and a copper thickness of 0.035 mm has used to fabricate the proposed sample. The copper-covered dielectric layer has been processed and discriminated from undesired metallic parts for both sides. Hence, the resonator part of the structure is obtained. The fabricated sample and measurement setup for the mentioned frequency range are shown in figure 1e. The simulations are realized by CST Microwave Studio under the same boundary conditions. The measurements are realized by measuring all the co-polar and cross-polar transmission and reflection values for the case of x- and y-polarized-incident waves by using a vector network analyser and two horn antennas (figure 1d). All the measurement results are calibrated for the free space conditions. The measurement and simulation results of linearly and circularly normalized-asymmetric transmission values are in good agreement as shown in figure 3. The exact linear asymmetry is observed at the frequency of 5.2 GHz. This

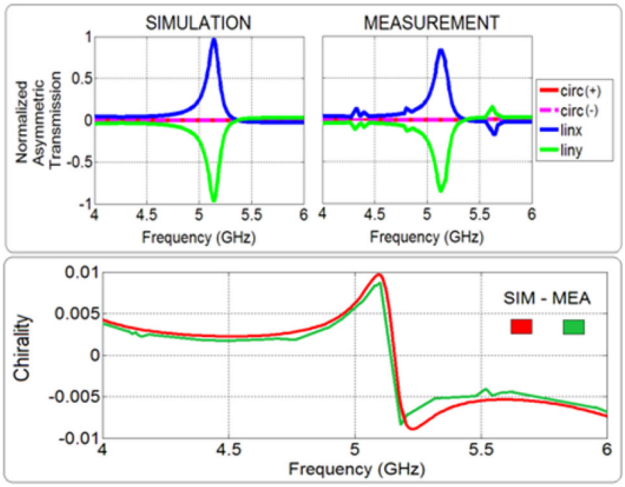

Figure 3. Asymmetric transmission and natural chirality parameters for linear and circular polarizations for the simulation and measurement results, respectively.

linear asymmetry results in a peak value of chirality (0.01) at the same frequency point. The correspondence of linear asymmetry and chirality confirm each other. Besides, the observed chirality values of the proposed π-shaped structure are in the range of chirality of natural chiral materials (figure 3). The most remarkable observation is the stability of the chirality between the ranges of 4.2–4.8 and 5.4–5.7 GHz. This property of the π-shaped structure offers researchers new opportunities such as equal amounts of polarization conversion and sensing applications within a wide frequency band.

It is well known that the asymmetric geometry of the structures placed on each side of a dielectric layer is the most common example of chiral MTMs. Due to the asymmetry of the π-shaped inclusions, the proposed structure demonstrates chirality [23–27]. Besides, the real part of the chirality (as shown in equation (6)) is directly related to the phase difference between the transmission coefficients of RCP (arg $(T+)$) and LCP (arg $(T-)$) waves. In the case of small chirality, low values of this difference in a wide range give rise to constant chirality in the same frequency spectrum.

3. Evaluation study with chiral MTM

3.1 *Proposed design and numerical setup (8–24 GHz regime)*

The proposed chiral MTM design consists of a π-shaped resonator on the front side and a rotated (30°) π-shaped resonator on the back-side as shown in figure 4. In addition, numerical calculations are analysed with CST Microwave Studio. Unit cell $(x-y)$ and open add space (z) boundary conditions are assigned in the simulation as mentioned before (figure 4a). Metallic resonators are modelled as the copper sheet with an

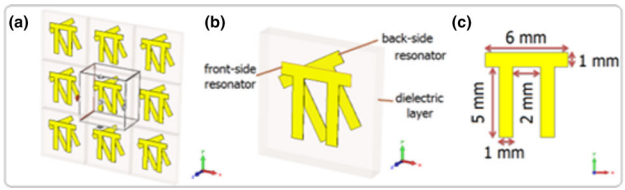

Figure 4. The suggested chiral MTM: (**a**) schematic view of the unit cell, (**b**) boundary conditions and (**c**) resonator.

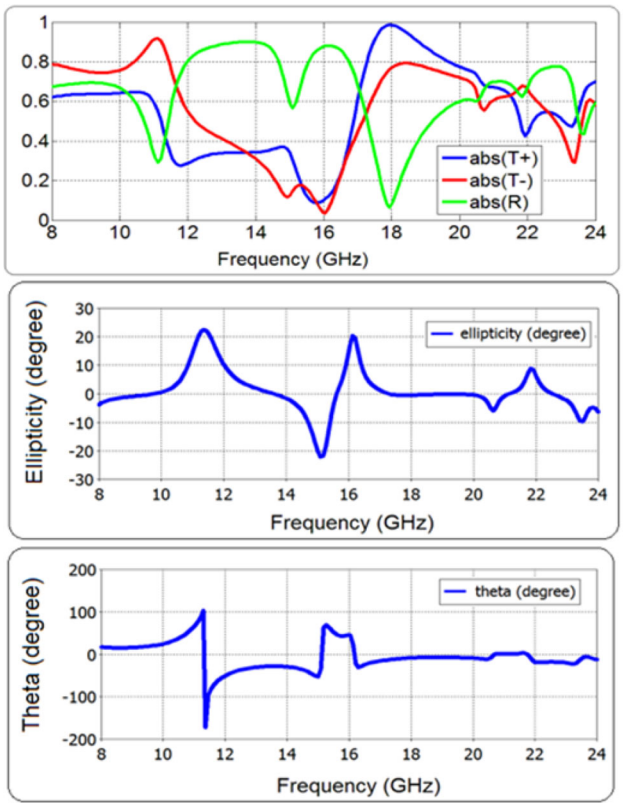

Figure 5. Transmission and reflection values, ellipticity and $\theta(^\circ)$ of the proposed structure, respectively.

electrical conductivity of $5.8001 \times 10^7\ \mathrm{S\,m^{-1}}$ and a thickness of 0.035 mm. Also, figure 4b and c shows side views and dimensions of the unit cell for the proposed structure.

The circular polarization components of transmission $T+/T-$ and reflection coefficients are extracted from the retrieval equations as a function of co-polar and cross-polar transmission values (equations (7) and (8)). It seems that 8–24 GHz ranges are observed between $T+$ and $T-$ values (figure 5). The variation of the transmitted wave polarization in the case of linearly polarized wave depending on the proposed asymmetric π-shaped model is evaluated with polarization azimuth rotation and ellipticity.

$$\eta = \frac{1}{2}\tan^{-1}\left(\frac{|T_+|^2 - |T_-|^2}{|T_+|^2 + |T_-|^2}\right), \tag{7}$$

$$\theta = \frac{1}{2}\delta = \frac{1}{2}\arcsin\left[\arg(T_+) - \arg(T_-)\right]. \tag{8}$$

At the resonance frequencies of 11.8, 15 and 16 GHz, both the azimuth rotation angle and ellipticity are at the peak points ($\eta = 22^\circ, \theta = -180^\circ$), ($\eta = -21^\circ, \theta = 80^\circ$) and ($\eta = 20^\circ, \theta = 60^\circ$), respectively. It means that the linearly polarized incident wave is converted to the elliptical wave with a strong distortion. At the frequency of 13.8 GHz, while ellipticity is around 0°, very good polarization rotation is observed ($\theta = 30^\circ$) with nearly zero dichroism. The sign change of the ellipticity in many frequency points provides a change in the polarization of the incident linear wave to RCP/LCP waves in a large frequency region (figure 5).

For waves propagating in the forward or backward direction, a slab of reciprocal chiral material appears completely identical. One supposes the schema of a circularly polarized plane wave normally incidents on the chiral MTM slab which has the thickness d, refractive index $n_\mp$ and impedance $Z = \sqrt{\mu/\varepsilon}$. In this instance, $T_\mp$ and $R_\mp$ are the amplitudes of the transmitted and reflected waves, respectively. $T'_\mp$ and $R'_\mp$ are the forward and backward propagating waves inside the slab. Now, when one implements the condition of continuity of tangential electric and magnetic fields ($z = 0$ and $z = d$), the following equation is obtained:

$$1 + R_\mp = T'_\mp + R'_\mp, \tag{9a}$$

$$1 - R_\mp = \frac{T'_\mp - R'_\mp}{Z}, \tag{9b}$$

$$T'_\mp e^{ik_\mp d} + R'_\mp e^{-ik_\mp d} = T_\mp, \tag{9c}$$

$$\frac{T'_\mp e^{ik_\mp d} + R'_\mp, e^{-ik_\mp d}}{Z} = T_\mp \tag{9d}$$

where $k_\mp = k_0(n \mp \kappa)$ is the wave vector. Then, eliminating $T'_\mp$ and $R'_\mp$ in equation (9), the transmission and reflection coefficients are obtained in following equations:

$$T_\mp = \frac{4Ze^{ink_0d}e^{\mp i\kappa k_0 d}}{(1+Z)^2 - (1-Z)^2 e^{2ink_0d}}, \tag{10a}$$

$$R_\mp = \frac{\left(1+Z^2\right)\left(e^{2ink_0d} - 1\right)}{(1+Z)^2 - (1-Z)^2 e^{2ink_0d}}, \tag{10b}$$

where both the reflections of the single slab should be the same. Inverting the above equation (10), the impedance Z and refractive index $n_\mp$ are given in equation (11) as shown below:

$$-Z = \mp\sqrt{\frac{(1+R)^2 - T_+T_-}{(1-R)^2 - T_+T_-}}, \tag{11a}$$

$$n_\mp = \frac{i}{k_0 d}\left\{\ln\left[\frac{1}{T_\mp}\left(1 - \frac{Z-1}{Z-1}R\right)\right] \mp 2m\pi\right\}, \tag{11b}$$

where m is an integer determined by the branches, $n_\pm = n \pm \kappa$, $\varepsilon = n/z$ and $\mu = nz$. Here, the effective medium

parameters can be evaluated by using retrieval equations [23–25,28,29]. Besides, the choice of m is realized to obtain physically meaningful results of the refractive index by using Kramers–Kronig relations. The effective medium parameters of the chiral MTM composed of π-shaped structures are shown in figure 6. Whereas the effective refractive index of the RCP wave ($n+$) have a strong response at the first resonance frequency (11.8 GHz) and goes negative, that of the LCP wave ($n-$) does not change abruptly and it is positive up to 14.5 GHz. The effective refractive index of the RCP wave ($n+$) has another peak at around the second resonance frequency and that of the LCP wave ($n-$) is zero. In contrast to the first and second resonance frequencies, the effective refractive index of the LCP wave ($n-$) shows a peak and that of the RCP wave ($n+$) goes to zero at around the third resonance frequency. It can be easily concluded that whereas the first negative value of the refractive index is caused by the signature of the conventional negative index MTM and the second negative value of the refractive index is resulted from the strong chirality of the π-shaped structure. Another important phenomenon about chiral MTMs, which is not emphasized before, is chiral nihility. This point is another important feature of the proposed π-shaped model. Whereas both effective permittivity and permeability are simultaneously zero, chirality is around 3 at the frequency of 15 GHz. Hence, the structure does not only propose strong chirality, polarization conversion and physical mechanism same as other conventional chiral MTMs, it also proposes chiral nihility within the same frequency band. It can be said that the proposed structure is a multifunctional one.

As the last step, the FOM and the effect of the backward resonator angle are also investigated [25,28,29]. It can be concluded that at the frequencies of the peak values of chirality, the performance of the structure is sufficient. Hence, the structure can be used as a polarizer especially at around 11.8 and 15 GHz (figure 6). The effect of the backward resonator angle on chirality is also investigated as shown in figure 7. Chirality is around zero for 0 and 180° due to the lack of asymmetry. Besides, strong optical activity is observed for intermediate values. Each structure with different backward angles has two strong chirality regions. The first one has negative chirality values. It has been narrowing up to 90° and positive for upper backward resonator angles.

3.2 *Numerical and experimental study for differences between chiral inclusions (4–6 GHz regime)*

The realization of the proposed asymmetric π-shaped chiral MTMs is investigated both numerically and experimentally in the range of our capability between the frequency bands of 4–6 GHz. All the material properties of dielectric, metal and backward-side resonator angles are the same with the structure studied between the frequency ranging from 8–24 GHz. The experimental studies have been achieved by using a vector network analyser. The proposed structure has placed between the two horn antennas and the transmission coefficients have been obtained. Firstly, the horn antennas

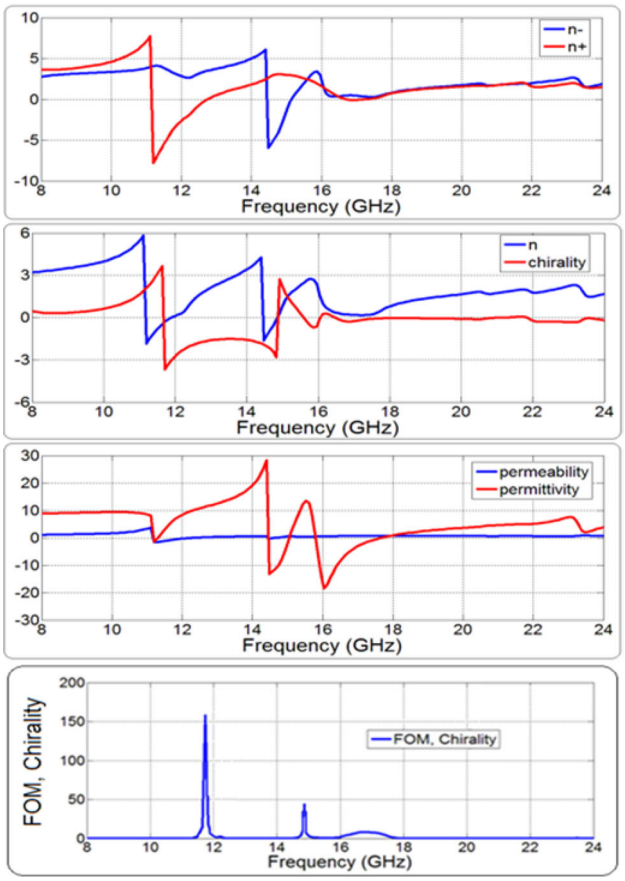

Figure 6. Retrieval results of the proposed structure.

have been arranged in the same polarization angle to monitor the co-polar transmission coefficient. Then, one of the antennas has been rotated by 90° to observe the cross-polarization transmission coefficient. Finally, the measured co-polar and cross-polar transmission coefficients have been evaluated by using equations from (4) to (11).

The simulation and measurement results of reflection and RCP/LCP transmission components from the suggested π-structure are in a good agreement as shown in figure 7. The ellipticity is around 0 in the frequency range from 4.5 to 5.5 GHz, due to the equal values of abs($T+$) and abs($T-$). There is only one resonance corresponding to a peak at around 4.3 GHz in the transmission spectrum which results from the differences between RCP and LCP transmission components. At the resonance, the transmission of the RCP is larger than that of the LCP. The observed peak is caused by the decrease in impedance mismatch induced by the strong electric/magnetic response for either RCP or LCP transmission. As mentioned before, the difference between the RCP and LCP transmission coefficients is denoted by ellipticity. In particular, the reason is that the RCP transmission is around 0.6 and the LCP transmission is very low, and the high difference value between them results in an ellipticity peak. The higher transmission is directly related to impedance match of free

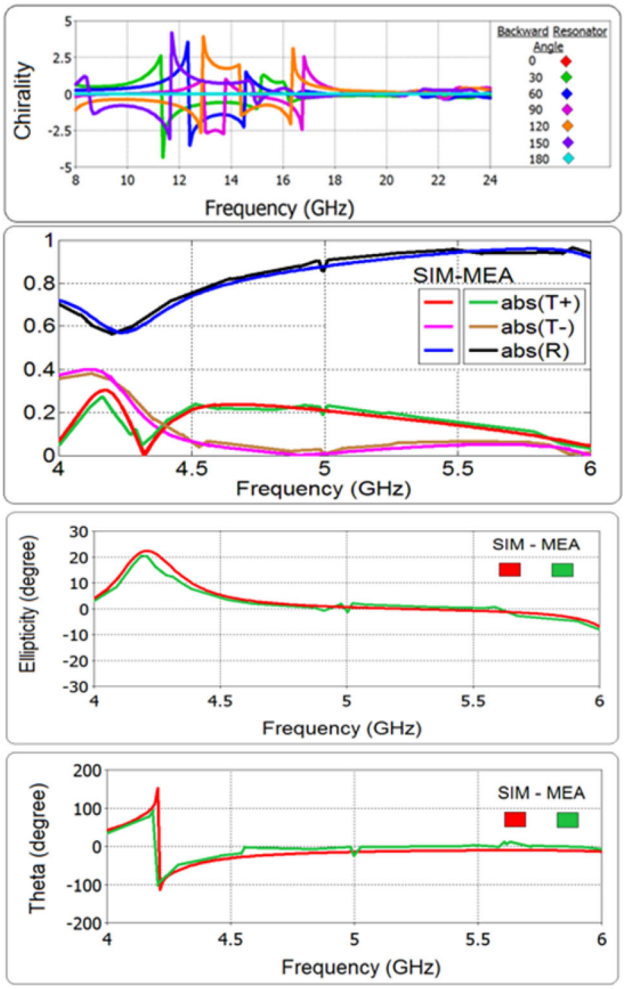

Figure 7. Chirality for different backward resonator angles, the transmission and reflection values, ellipticity and θ (°) of the proposed structure, respectively.

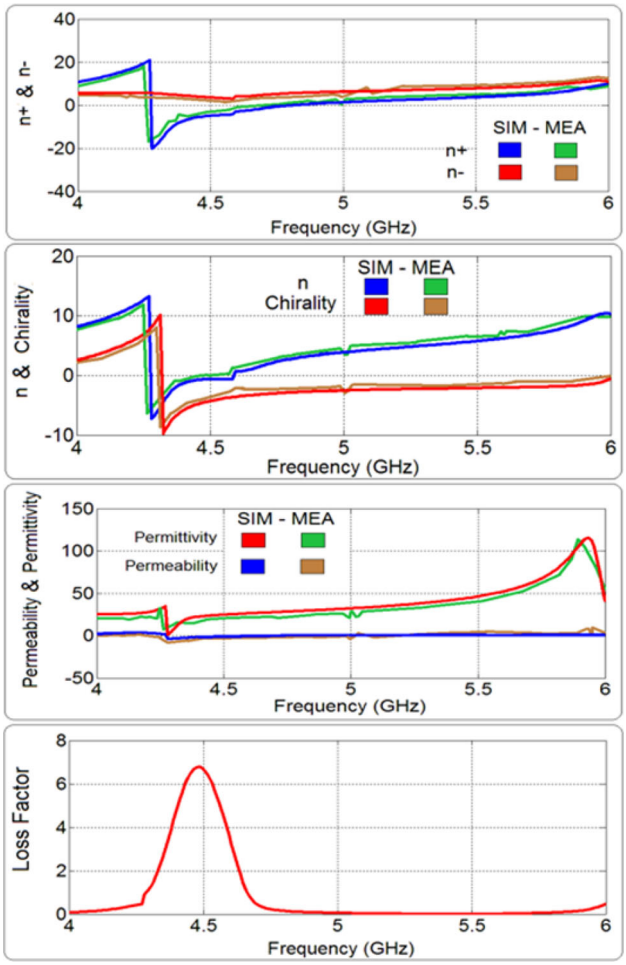

Figure 8. Retrieval results of the proposed structure.

space and π-shaped-chiral MTMs. It can be concluded that a good ellipticity needs difference between circularly polarized components of a transmitted wave. It can be provided by a good or worse impedance match between free space and chiral medium for RCP and LCP transmissions. The mismatch is due to the strong electric or magnetic response of the inclusions. At the resonance frequency, the linearly polarized-incident wave is modified to a strong distortional elliptical wave with an angle of 22° (figure 7). The rotator power (θ) denotes differences in the phases of RCP and LCP components of transmission. Far from the resonance frequency, the phases of circularly polarized-components have to be similar. Besides, near resonance frequencies, phases of RCP and LCP differ certainly and the linearly polarized-incident wave propagating towards chiral MTMs is rotated by an angle of $-100°$ (figure 8).

Effective medium parameters of the π-shaped structures between frequencies of 4–6 GHz are obtained both numerically and experimentally as shown in figure 8. While, a strong response has been observed at around the resonance frequency of 4.3 GHz and goes positive for the effective refractive index of the RCP wave ($n+$), that of the of the LCP wave ($n-$) is closely constant and positive for all frequency ranges. Since, the effective permittivity and permeability are not simultaneously negative. The negative effective refractive index is due to the strong optical activity between 4.3 and 4.6 GHz. A nearly constant value of strong chirality between 4.7 and 5.5 GHz is a fascinating and first debuting phenomenon in the literature. Hence, the study not only proposes constant natural chirality, but also suggests constant strong chirality. In addition, the LF of the proposed structure is in an acceptable range as shown in figure 8.

4. Conclusion

In conclusion, firstly, a new multi-functional chiral MTM is numerically designed and the optimum structure is found by genetic algorithm methods by using the commercial software, CST Microwave Studio. We tuned and optimized

dimensions of the resonator to obtain multi-band asymmetric transmission. The suggested optimized structure is investigated in detail. The proposed model consists of π-shaped resonators. It has a very simple configuration and fabrication techniques. Secondly, the suggested model is theoretically and numerically analysed, retrieved and evaluated. The obtained results show that the proposed model presents multi-band asymmetric transmission and small chirality. Usually, chiral MTM studies in the literature focus on large chirality. However, this study introduces a new type of chiral MTM which has small chirality like a natural chiral medium and chiral nihility MTM. Furthermore, it guides to design new polarization rotator devices to be used in myriad potential applications. Although the concept seems similar to the studies in the literature, it is the first study on chiral MTMs to realize the nihility. Also, there are limited numbers of studies investigating natural chirality with the MTM concept.

As mentioned in the study, the structures are both asymmetric and have high chirality. Besides, the structure also exhibits natural chirality depending on the angle between front- and back-side inclusions. Hence, the mentioned structure can be used to realize both high and very small natural chirality values depending on the angular dependencies of the inclusions placed on front- and back-sides. The higher chirality value is due to the asymmetry between co-polar and cross-polar transmitted values of the electric field. Since, it can be concluded that the increment of the difference between $T+$ and $T-$ values, results in higher chirality. Besides, unexpected values of chirality are due to the lack of asymmetry.

The study includes both numerical analysis and experimental validations. The numerically investigated structure is fabricated as can be seen in figure 1. Numerically extracted asymmetric transmission and chirality values are supported by experimental analysis as can be seen in figure 3. These values are critical for the study. In addition, the transmission and reflection values and ellipticity and $\theta(^\circ)$ of the proposed structure are also both numerically and experimentally investigated as can be seen in figure 7. Besides this, retrieval values of the structure are also compared with measured ones (figure 8). It is demonstrated that the proposed structure has a multi-band asymmetric transmission characteristic at the resonance frequencies of 10.85, 14.49 and 14.88 GHz, for linear polarization of the incident wave. In addition, a small natural chirality value can be obtained at the frequency of 16 GHz. The novelty of the study is the low values of chirality. Besides this, an exact linear asymmetry is observed at the frequency of 5.2 GHz with a small chirality value of 0.01. A frequency independent chirality is realized in the frequency ranges of 4.2–4.8 and 5.4–5.7 GHz. This property of the π-shaped structure offers researchers new opportunities such as an equal amount of polarization conversion and sensing applications within a wide frequency band. It is demonstrated that the π-shaped resonator can convert the linearly polarized-incident wave into the elliptical wave at the resonance frequencies of 11.8, 15 and 16 GHz with the azimuth rotation angle and ellipticity of ($\eta = 22^\circ$, $\theta = -180^\circ$), ($\eta = -21^\circ, \theta = 80^\circ$) and ($\eta = 20^\circ, \theta = 60^\circ$), respectively. The proposed simple sample not only provides constant small chirality, but also as constant strong chirality between 4.7 and 5.5 GHz which is a first debuting phenomenon in the literature. Hence, this study provides novelty for microwave power and energy since, radar applications include microwave power and polarization conversion of microwave provides the direction of microwave energy to the desired direction.

References

[1] Smith D R and Kroll N 2000 *Phys. Rev. Lett.* **85** 2933
[2] Wiltshire M C K, Pendry J B, Young I R, Larkman D J, Gilderdale D J and Hajnal J V 2001 *Science* **291** 84
[3] Akgol O, Unal E, Bağmancı M, Karaaslan M, Sevim U K, Ozturk M *et al* 2019 *J. Electron. Mater.* **48** 2469
[4] Ozturk M, Akgol O, Sevim U K, Karaaslan M, Demirci M and Unal E 2018 *Constr. Build. Mater.* **165** 58
[5] Yen T J, Padilla W J, Fang N, Vier D C, Smith D R, Pendry J B *et al* 2004 *Science* **303** 1494
[6] Akgol O, Bağmancı M, Karaaslan M and Ünal E 2017 *J. Microwave Power EA* **51** 134
[7] Tümkaya M A, Karaaslan M and Sabah C 2018 *Bull. Mater. Sci.* **41** 91
[8] Ozturk M, Sevim U K, Akgol O, Karaaslan M and Unal E 2019 *Measurements* **138** 356
[9] Sabah C, Tugrul T H, Dincer F, Delihacioglu K, Karaaslan M and Unal E 2013 *Prog. Electromagn. Res.* **138** 293
[10] Altintas O, Unal E, Akgol O, Karaaslan M, Karadag F and Sabah C 2017 *Mod. Phys. Lett. B* **31** 1750274
[11] Bakır M, Karaaslan M, Akgol O and Sabah C 2017 *Opt. Quant. Electron.* **49** 346
[12] Tang J, Xiao Z, Xu K, Ma X, Liu D and Wang Z 2016 *Opt. Quant. Electron.* **48** 111
[13] Xu K K, Xiao Z Y, Tang J Y, Zheng X X and Ling X Y 2016 In *progress in electromagnetic research symposium*, p 2713
[14] Sabah C and Roskos H G 2012 *Prog. Electromagn. Res.* **124** 301
[15] Mandatori A, Bertolotti M and Sibilia C 2007 *JOSA B* **24** 685
[16] Serebryannikov A E and Lakhtakia A 2013 *Opt. Lett.* **38** 3279
[17] Fedotov V A, Mladyonov P L, Prosvirnin S L, Rogacheva A V, Chen Y and Zheludev N I 2006 *Phys. Rev. Lett.* **97** 167401
[18] Menzel C, Helgert C, Rockstuhl C, Kley E B, Tünnermann A, Pertsch T *et al* 2010 *Phys. Rev. Lett.* **104** 253902
[19] Huang C, Feng Y, Zhao J, Wang Z and Jiang T 2012 *Phys. Rev.* **85** 195131
[20] Huang C, Zhao J, Jiang T and Feng Y 2012 *J. Electromagnet. Wave* **26** 1192
[21] Dincer F, Karaaslan M, Unal E, Delihacioglu K and Sabah C 2014 *Prog. Electromagn. Res.* **144** 123
[22] Plum E, Zhou J, Dong J, Fedotov V A, Koschny T, Soukoulis C M *et al* 2009 *Phys. Rev.* **79** 035407
[23] Wang B, Zhou J, Koschny T, Kafesaki M and Soukoulis C M 2006 *J. Opt. A-Pure Appl.* **11** 114003
[24] Plum E, Zhou J, Dong J, Fedotov V A, Koschny T, Soukoulis C M *et al* 2009 *Phys. Rev. B* **79** 035407
[25] Zhao R, Zhang L, Zhou J, Koschny T and Soukoulis C M 2011 *Phys. Rev. B* **83** 035105

[26] Zhao R, Koschny T and Soukoulis C M 2010 *Opt. Express* **18** 14553
[27] Ye Y and He S 2010 *Appl. Phys. Lett.* **96** 203501
[28] Li Z, Caglayan H, Colak E, Zhou J, Soukoulis C M and Ozbay E 2010 *Opt. Express* **18** 5375
[29] Li Z, Alici K B, Colak E and Ozbay E 2011 *Appl. Phys. Lett.* **98** 161907
[30] Sonsilphong A and Wongkasem N 2012 *Int. J. Phys. Sci.* **7** 2829
[31] Demarest K R 1997 *Engineering electromagnetics* (New Jersey: Prentice Hall) 1st edn
[32] Feynman R P, Leighton R B and Sands M 1963 *The Feynman lecture on physics* (Boston: Addison-Wesley Pub. Co.) 1st edn vol 1